

1 [RC1: 'Comment on bg-2023-2', Anonymous Referee #1, 14 Mar 2023](#) [reply](#)

2 General comments:

3 This well-written study presents work empirically determining the threshold of mobilisation  
4 for individual rubble pieces of varying shapes and sizes, and on different substrate types  
5 and slopes, in both controlled and field settings (the Maldives). Rubble movement is relevant  
6 because it impacts coral recovery, and many threats to coral (e.g. destructive fishing,  
7 storms, bleaching) result in coral breakage and/or death. These pieces become “rubble” of  
8 various sizes and shapes. The experiments are clever and thorough, designed to elucidate  
9 the probability of rubble ‘rocking’ or various types of ‘transport’ (walk/slide/flip).  
10 Unsurprisingly, the authors found similar mobilisation thresholds in the wave flume and in  
11 the field, and that the probability of rubble mobilisation increases with higher velocity. Also  
12 as common sense and previous work would suggest, it decreases as: (i) rubble size  
13 increases; (ii) morphological complexity/‘branchiness’ (of both the rubble and of the  
14 substrate type) increases; and (iii) as the slope angle decreases (and the contribution of  
15 gravity subsequently decreases). Interlocking and ‘settling’ of rubble was a strong inhibitor  
16 of mobilisation.

17 Specific comments

18 While the authors did find some some nuanced results (e.g. larger rubble is more likely to  
19 settle into sand) and differences between the northeastern and western monsoon seasons,  
20 overall, their results seem a very sophisticated experimental demonstration of what common  
21 sense would predict. While sentences in the Abstract (l 19–21) and Introduction (l 37–40)  
22 suggest relevance for managers of reefs that exhibit a significant increase in rubble cover,  
23 there is no discussion of what managers can actually do once they have the information  
24 presented herein. While there is mention of “rubble stabilisation interventions to enhance  
25 coral recruitment and binding,” it’s unclear that the results from this work would actually be  
26 needed to predict the likelihood of natural rubble stabilisation and recovery **beyond simple**  
27 **first principles**. I suggest the discussion at least address potential management relevance,  
28 including context for discussions for rubble stabilization, budget needed vs. scale of the  
29 problem, etc.

30 No technical corrections.

31 Our response:

32 We thank Reviewer 1 for their review of the manuscript and are pleased that they found the  
33 results to be novel yet intuitive. We thank the reviewer for their comment regarding  
34 highlighting potential management relevance, which is a valuable addition to the  
35 manuscript. The revised manuscript includes reference to management relevance in the  
36 introduction (as before), and in the discussion, pasted below and on line 642 of the revised  
37 manuscript (no track changes).

38 **“Implications for management**

39 “The scale of reef degradation and subsequent intervention methods is vast, putting pressure on reef restoration  
40 budgets. While operationalising the implementation of reef restoration at scale is investigated (Saunders et al.  
41 2020), tools that allow managers to prioritise reefs that are particularly vulnerable to rubble mobilisation, and thus  
42 longer natural recovery times, are essential (Kenyon et al. 2022). The results of this study provide information

43 toward improved management of damaged reefs with high rubble cover. Broadly, rubble stabilisation interventions  
44 might be considered at lower mobilisation thresholds if a rubble bed is composed mostly of loose (not interlocked),  
45 small pieces, particularly with low morphological complexity, which is more commonly the case with  
46 anthropogenic disturbances such as ship groundings, human trampling, coastal armouring and blast fishing  
47 (Masucci et al. 2021, Kenyon et al. 2022). More comprehensively, the mobilisation estimates reported here can  
48 be used in modelling frameworks that predict the frequency of everyday rubble mobilisation in a certain location,  
49 based on a modelled time series of wave climate estimates, such as the developed everyday wave conditions model  
50 for the Great Barrier Reef (Roelfsema et al. 2020). Reefs or areas of reefs at higher risk of frequent rubble  
51 mobilisation can be prioritised for rubble stabilisation interventions following disturbances, with predictions being  
52 improved through consideration of the mobilisation processes discussed, e.g., settling and interlocking over time;  
53 bathymetry; rubble quantity, size and morphology (driven by disturbance, surrounding coral cover and diversity);  
54 water quality and bioerosion.”  
55

56 **Citation:** <https://doi.org/10.5194/bg-2023-2-RC1>

57 **RC2:** '[Comment on bg-2023-2](#)', Anonymous Referee #2, 31 May 2023 [reply](#)

58 **General comments**

59 This manuscript describes an interesting study of movement of coral rubble under waves.  
60 The lab and field measurements of rubble movement seem to have been generally well-  
61 executed, the combination of lab and field measurements is informative, the figures show  
62 interesting patterns, and the datasets have a lot of potential. While I think the manuscript  
63 has potential to ultimately be a nice contribution, I do have serious concerns about aspects  
64 of the analysis and the way some of the methods and results are presented in this  
65 submission. My major concerns are around the treatment of wave period, which is very  
66 different (factor of up to 10) in the lab versus in the field, and the use of orbital velocity as  
67 the hydrodynamic parameter against which rubble movement is plotted and assessed.

68 The physics of rubble motion under waves isn't fully explained in the manuscript so I  
69 provide some background here. The total force on an object under waves is the sum of two  
70 components: the inertial force and the drag force. The drag force is proportional to orbital  
71 velocity squared and dominates only if the orbital excursion is substantially larger than the  
72 size of the object (Keulegan Carpenter number  $KC > 1$ ). From my back-of-the-envelope  
73 calculations this seems to be the case in much of the field data presented. However, if the  
74 orbital excursion is smaller than the object size ( $KC < 1$ ), the inertial force is the dominant  
75 force on the obstacle. The inertial force is proportion to the fluid ACCELERATION, which is  
76 the orbital velocity multiplied by the wave frequency ( $2\pi / \text{PERIOD}$ ). By my calculations the  
77 inertial force should be the dominant force for many of the lab flume conditions. The wave  
78 period is therefore a critical parameter for this problem, in addition to the orbital velocity.

79 Because of the very different wave periods between the lab and the field, comparisons  
80 between the two datasets need to be done very carefully/cautiously. Additionally, in the lab  
81 flume, it seems the period was changed (somewhat arbitrarily when breaking was observed),  
82 but the combinations of wave height and period are not reported in the manuscript. A table  
83 of the combinations of conditions in the lab flume experiments needs to be reported, along  
84 with corresponding bottom orbital excursions, velocities, accelerations. This will allow  
85 comparison of orbital excursions with rubble sizes which will inform as to whether drag  
86 (proportional to velocity squared) or inertial force (proportional to acceleration) is the  
87 relevant force. Ideally, the probability of movement would be plotted against a measure of  
88 the total force rather than velocity. There is a nice paper by Viehman et al. (2018) that lays

89 out these forces on rubble. It is cited briefly in the introduction, but I think it could be a  
90 useful reference for sorting out this issue of dominant forces.

91 The figures are generally well-constructed and the manuscript text is well-organized and  
92 generally well-written.

93 I provide a few specific comments below, but I have not provided line-by-line comments at  
94 this point because of the critical major issues described above.

95 Our response:

96 We thank Reviewer 2 for their review of the manuscript and the time taken to provide  
97 comments. We thank the reviewer for their queries in relation to the methodology, which  
98 has led to an improved manuscript through inclusion of additional information, though we  
99 note that the results do not change substantially. We believe the review comments regarding  
100 inertial forces are due to an omission on our part in the original manuscript, where the coral  
101 diameter was never stated. Consequently, we believe the reviewer may have anticipated  
102 significant inertia forces in the laboratory assuming coral diameters of 0.04–0.2 m, instead  
103 of coral diameters of 0.01–0.02 m. The reviewer is correct that coral diameters of the  
104 former size range would lead to significant inertia forces. We apologise that the coral  
105 diameter was not previously included in the original manuscript, but rather only the lengths  
106 were specified.

107 The actual coral diameters used in the lab do not lead to significant inertia forces for the  
108 wave conditions that lead to rubble movement. This is addressed at length in these  
109 comments, where we have derived a new relationship for the contribution of the inertia  
110 force to the total maximum force as a proportion of the drag force. We have included a table  
111 of wave conditions used in the flume (Table S1 – line 35) and the field (Table S2 – line 42) in  
112 the revised Supplementary Material. These show the average coral rubble diameter,  
113 significant wave height, period, water depth, and corresponding velocities, inertia force  
114 component and bottom orbital excursions for all wave conditions used in determining the  
115 relationship between velocity and movement.

116 These tables highlight in which conditions there is potential for the inertia force to be the  
117 dominant force as opposed to drag, based on an average coral diameter of 1.64 cm (range  
118 ~1–2 cm) in the flume and 1.69 cm (range ~1–3 cm) in the field. The calculations are  
119 outlined below.

120 Assuming the drag and inertia coefficients have the same magnitude, the ratio of the  
121 maximum inertia force to the maximum drag force is given by Dean and Dalrymple (1991)  
122 as:

123  $\frac{F_I}{F_D} = \frac{\pi^2}{KC} = \alpha$  where  $KC = \frac{uT}{\phi}$ ;  $KC = Keulegan-Carpenter number$ ,  $u = maximum orbital$   
124  $wave\ velocity$ ,  $T = wave\ period$   $\phi = rubble\ diameter$

125 Hence  $F_I = \alpha F_D$

126 The maximum total force is again given by Dean and Dalrymple (1991), noting that the drag  
127 and inertia forces are out of phase,

128  $F_T = F_D + \frac{F_I^2}{4.F_D}$   $F_T = \text{maximum total force, } F_D = \text{drag force, } F_I = \text{inertia force}$

129 *which can be written as*

130  $F_T = F_D + \frac{\alpha^2}{4} F_D$

131 *or*

132  $F_T = F_D + \frac{24}{KC^2} F_D$

133 The last term ( $\frac{24}{KC^2}$ ) gives the contribution of the inertia force to the total maximum force as a  
134 proportion of the drag force. This inertia component is shown in the second- and third-last  
135 columns of Tables S1 and S2.

136 When the inertia component ( $\frac{24}{KC^2}$ ) contributes more than 25% of the drag force to the total  
137 force, we consider that to be a potentially significant contribution. For example, when  $F_I = F_D$ ,  
138 the contribution to the maximum total force from the inertia force is  $0.25F_D$ . It should be  
139 noted that this relationship is only valid for  $\frac{F_I}{F_D} < 2$ , and when  $\frac{F_I}{F_D} > 2$ , the maximum force is  
140 pure inertia, meaning it is the dominant force (Dean and Dalrymple, 1991). The maximum  
141 force is shown in the last column of Tables S1 and S2.

142 Table S1 (line 35) shows that only 18 out of 71 wave conditions in the flume have the  
143 potential for the inertia force to be significant, and of those, only 6 had a  $\frac{F_I}{F_D}$  ratio  $> 2$ ,  
144 meaning that nearly all the wave conditions in the flume led to drag-dominated conditions.  
145 Table S2 (line 42), confirms that only 1 out of 90 wave conditions in the field had the  
146 potential for inertia to be significant. This condition corresponded to a very low velocity  
147 (0.016 m/s), far from the reported transport threshold velocities. Thus, further  
148 investigations were made for flume conditions (see below) but not field conditions.

149 The above calculations were applied to the dataset used to determine the probabilities of  
150 rocking, flipping and transport in the flume (for loose and interlocked rubble), so that each  
151 individual rubble piece's diameter could be used in place of the average diameter of  
152 1.64 cm. Figure S5 (line 15) shows the relationship between bottom orbital velocity and the  
153  $F_I/F_D$  ratio for every individual case in the flume. There is a general trend in which  $F_I/F_D$   
154 decreases as both velocity and the likelihood of movement increases. The dataset includes  
155 7,593 rows and of these, 2,081 had the potential for inertia forces to be significant based  
156 on the above calculations. However, in most (90%) of the 2,081 identified cases, there was  
157 no movement of the rubble being tested (Figure S8 - line 26).

158 In 9.3% of cases (195 of 2,081), rocking movements only were recorded (Figure S6 - line  
159 19). For these cases, the contribution of inertia force to the total force ranged from 25% to  
160 100% or more of that contributed by the drag force. The highest velocity represented in  
161 these cases was 0.2 m/s, though the large majority were much lower. Thus, at velocities  
162  $< 0.2$  m/s, there is the potential for inertia forces to contribute to causing rocking motions.  
163 But, at a velocity of 0.2 m/s the contribution of inertia is still only 25% of the drag force (not  
164 dominant). This is now indicated in the caption for the plot of velocity vs probability of  
165 rocking (Figure 3a) in the revised manuscript (line 351) and as pasted below:

166 “Figure 3: The probability of (a) rocking, (b) transport, and (c) flipping with increasing near-bed wave orbital  
167 velocity for branched and unbranched rubble of four size categories (grey: 4-8 cm; green: 9-15 cm; light blue: 16-22  
168 cm; dark blue 24-39 cm) on rubble and sand substrates. Note that at low velocities  $<0.2$  m/s, we estimate there is the  
169 potential for inertia forces to contribute to causing rocking motions; and at velocities  $<0.16$  m/s, there is the potential  
170 for inertia forces to contribute to causing transport and flipping.”

171 In any case, these instances of ‘rocking’ were considered as ‘no movement’ in the analysis  
172 determining the probability of transport (see Table 1 of the manuscript) and thus have no  
173 bearing on the 50% or 90% thresholds of transport reported.

174 Only in 0.9% of the cases where inertia forces were potentially significant (18 of 2,081), was  
175 transport/flipping recorded (Figure S6 – line 19). For these cases, the average contribution  
176 of inertia forces to the total force was 36% of the drag force (Figure S7 – line 23). The  
177 highest velocity represented in these cases was 0.16 m/s (Figure S6 – line 19). This indicates  
178 that at very low velocities  $<0.16$  m/s, there is the potential for inertia forces to be  
179 significant. However, this cut-off is well below the 50% and 90% thresholds of transport that  
180 are reported in the paper, and at those velocities, i.e.,  $\geq 0.3$  m/s, the inertia component  
181 contributes as little as 0.1% and at most 4.9% to the total force, and the threshold of motion  
182 conditions are thus drag dominated (Figure S8 – line 26).

183 The reviewer also states that “ideally, the probability of movement would be plotted against  
184 a measure of the total force rather than velocity”. We disagree that this is necessary, based  
185 on the above calculations and justification, which are included in Supplementary Material  
186 and text included in the revised manuscript. The total force is also directly dependent on the  
187 length of the coral rubble pieces. The threshold of motion is not directly dependent on that  
188 length, since, for a given velocity, doubling the length doubles both the force and the  
189 resisting force. The observed thresholds are indirectly influenced by length through the  
190 greater probability of a longer length piece having a shape that is more stable due to  
191 curvature or branches. Furthermore, we feel a plot of movement against velocity is more  
192 widely interpretable to a broad coral reef scientist audience, rather than only to those with a  
193 knowledge of sediment transport and hydrodynamics, as flow speed is commonly measured  
194 on reefs while forces are not. However, we do include tables showing the inertial force  
195 component for each velocity (Tables S1 and S2), and plots of how the inertia force  
196 component changes with velocity and movement (Figures S5 and S8, lines 15 and 26) in the  
197 Supplementary Material.

198 To incorporate the above response into the revised manuscript we have included the  
199 following sections, with line numbers corresponding to the manuscript with *no* track  
200 changes.

201 Section 2.1 (Line 158)

202 “To determine whether scaling effects were necessary to compare velocity thresholds between flume and field  
203 conditions, we derived a relationship for the contribution of the inertia force to the total maximum force as a  
204 proportion of the drag force, for all wave conditions for each run. Total force depends on both the inertia force  
205 and drag force components, and while the inertia component is dependent on velocity and wave period, the drag  
206 component is solely dependant on velocity (Table S1). Thus, where conditions are determined to be drag  
207 dominated, rubble movement depends primarily on velocity, and valid comparisons between flume and field can  
208 be made despite their variance in wave period.

209 The inertia component and maximum force for each wave height and period combination in the flume, based on  
210 an average coral diameter of 1.64 cm (range  $\sim 1$ -2 cm), are shown in Table S1. Only 19 out of 71 wave

211 conditions in the flume have the potential for the inertia force to be significant, and of those, only 7 had a  $\frac{F_I}{F_D}$   
212 ratio  $>2$ , meaning that nearly all wave conditions in the flume led to drag-dominated conditions. Furthermore,  
213 the inertial component decreases as velocity increases (Figure S5), and inertial forces were negligible at the 50%  
214 and 90% thresholds (see results for further explanation). The flume and field experiments are therefore  
215 comparable without scaling effects.”

216 Section 2.2 (Line 211)

217 “The contribution of the inertia force to the total maximum force as a proportion of the drag force was estimated  
218 for each  $H_s$  and  $T_p$  combination used in the field analysis, based on an average coral diameter of 1.69 cm (range  
219 ~1-3 cm) (Table S2). Only 1 out of 90 wave conditions in the field had the potential for inertia to be significant,  
220 meaning that most conditions in the field were drag-dominated. Furthermore, this one condition corresponded to  
221 a very low velocity (0.016 m/s), far from the reported 50% and 90% transport threshold velocities.”  
222

223 Section 3.1.1 (Line 323)

224 “As well as calculating the inertia component for each wave height and period combination in the flume based on  
225 the average coral diameter (see 2.1 Methods), we also made these calculations for individual runs using the unique  
226 diameter of each piece. Of the cases identified as having the potential for inertia forces to be significant, 9.3%  
227 (195 of 2,081) were runs where only rocking movements were recorded. The highest velocity represented in these  
228 cases was 0.2 m/s, though the large majority were much lower (Figure S6). Thus, at velocities  $<0.2$  m/s, there is  
229 the potential for inertia forces to contribute to causing rocking motions. But, at a velocity of 0.2 m/s the  
230 contribution of inertia is still only 25% of the drag force (not dominant), and the threshold of rocking conditions  
231 in the flume, reported above, are drag dominated.

232 Transport or flipping occurred in only 0.9% of runs where we determined inertia forces to be potentially significant  
233 (18 of 2,081 runs) (Figure S7). For these cases, the average contribution of inertia forces to the total force was  
234 36% of the drag force and the highest velocity represented in these cases was 0.16 m/s (Table S7). This indicates  
235 that at low velocities  $<0.16$  m/s, there is the potential for inertia forces to be significant. However, this cut-off is  
236 well below the 50% and 90% thresholds of transport reported above, and at those velocities the inertia component  
237 contributes as little as 0.1% and at most 4.9% to the total force. The threshold of transport conditions in the flume  
238 are thus drag dominated.”

239 We have also included description of the equations used to calculate inertia force in the  
240 Supplementary Material on line 34 and pasted below.

**Table S1/S2 pre-amble:** Assuming the drag and inertia coefficients have the same magnitude, the ratio of the maximum inertia force to the maximum drag force is given by Dean and Dalrymple (1991) as:

$$(1) \frac{F_I}{F_D} = \frac{\pi^2}{KC} = \alpha \quad \text{where } KC = \frac{uT}{\phi}; \text{ KC = Keulegan-Carpenter number, } u = \text{maximum orbital wave velocity, } T = \text{wave period } \phi = \text{rubble diameter}$$

Hence  $F_I = \alpha F_D$

The maximum total force is again given by Dean and Dalrymple (1991), noting that the drag and inertia forces are out of phase,

$$(2) F_T = F_D + \frac{F_I^2}{4F_D} \quad F_T = \text{maximum total force, } F_D = \text{drag force, } F_I = \text{inertia force}$$

which can be written as  $F_T = F_D + \frac{\alpha^2}{4} F_D$  or  $F_T = F_D + \frac{24}{KC^2} F_D$

The last term ( $\frac{24}{KC^2}$ ) gives the contribution of the inertia force to the total maximum force as a proportion of the drag force. We consider the inertia component to be potentially significant when it contributes more than 25% of the drag force to the total force. For example, when  $F_I = F_D$ , the contribution to the maximum total force from the inertia force is 0.25 $F_D$ . It should be noted that this relationship is only valid for  $\frac{F_I}{F_D} < 2$ , and when  $\frac{F_I}{F_D} > 2$ , the maximum force is pure inertia (Dean and Dalrymple, 1991).

241

242 **Specific comments**

243 Abstract lines 10–15, and corresponding sections of the text. Comparisons rubble motion in  
 244 lab and field studies with respect to orbital velocities are flawed, due to the reasons outlined  
 245 above in my general comments. Also, rubble size is an important determinant of when  
 246 motion occurs, so I didn't understand why a single probability of motion at a single velocity  
 247 was reported.

248 Diagram – the statement that rubble is mobilized for orbital velocities greater than 0.4 m/s  
 249 is too simplistic since we know (and the results show) there is a strong dependence on  
 250 rubble size. There will also be a dependence on wave period for some rubble size classes  
 251 and wave conditions due to inertial force being the dominant force.

252 We thank the reviewer for these more detailed comments. As described above, the  
 253 comparisons between flume and field are made with respect to the 50% and 90% thresholds  
 254 of transport, and at those velocities, i.e., 50% at  $\geq 0.3$  m/s, the inertia component  
 255 contributes as little as 0.1% and at most 4.9% to the total force in the flume (Figure S8 – line  
 256 26), and conditions are thus drag dominated. At and above this same velocity threshold in  
 257 the field, the inertia component contributes on average 0.08% and a maximum of 1% to the  
 258 total force (Table S2). Thus, comparisons between flume and field are valid despite  
 259 differences in wave period. With respect to variation in rubble length, the graphical abstract  
 260 is a summary of the information provided in the paper, and the value given is the 90%  
 261 threshold averaged across substrates, morphologies and rubble lengths from 4–23 cm (and  
 262 diameters  $\sim 1$ –3 cm). This has now been highlighted in the footnote of the graphical abstract  
 263 which can be seen on line 38 of the revised manuscript and pasted below.

264 “50% chance of movement averaged across substrate, rubble morphology, rubble lengths 4-23 cm & diameters  
 265  $\sim 1$ -3 cm”

266 The figures in the manuscript provide the detail around rubble movement with respect to  
267 varying rubble lengths and morphologies, and we note in the discussion that "...interventions  
268 might be considered at lower mobilisation thresholds (e.g., 50% of 4-8 cm unbranched rubble predicted to move  
269 at 0.14 m/s in the field; Figure 6a) if a rubble bed is comprised predominantly of very small pieces" (Line 567).  
270 Additional supplementary tables of model predictions for figures can be included if  
271 additional detail is desired.

272 Page 6, line 5–10. A table of wave conditions in the flume (height, period, water depth) is  
273 needed. The description of how wave period was increased when waves started to break  
274 seems very arbitrary. Changing the wave period for the same wave height will alter the  
275 orbital velocity, orbital excursion, and acceleration.

276 Linear wave theory and the Soulsby model are less accurate once wave breaking occurs.  
277 Breaking wave conditions were thus avoided by changing the wave conditions to reduce the  
278 wave steepness. This alters the orbital velocity and forces, but has no bearing on the  
279 analysis, merely the order in which different conditions are achieved.

280 We have included a table of wave conditions used in the flume in the Supplementary Material  
281 (Table S1 – line 35). These show the average coral rubble diameter, significant wave height,  
282 period, water depth, and corresponding velocities, inertia force component and bottom  
283 orbital excursions for all wave conditions used in determining the relationship between  
284 velocity and movement.

285 P6, Line 17–20. Linear wave theory is generally used to estimate bottom orbital velocities,  
286 accelerations, excursions. The approach described here (Soulsby cosine approximation) is  
287 non-standard and I didn't understand why it was used in preference to linear wave theory.

288 The Soulsby cosine approximation is a one-step method to estimate bottom orbital velocity  
289 without solving the dispersion relationship, thus it was simpler to implement. A comparison  
290 of bottom orbital velocities estimated from linear wave theory compared to the Soulsby  
291 cosine approximation was conducted prior to submission of the original manuscript, for the  
292 wave conditions used in the flume. This relationship is shown in Figure S2 (line 4) of the  
293 Supplementary Material.

294 Velocities were found to be almost identical between methods, with an average change of  
295 0.4 cm/s (55% <0.5 cm/s difference, 90% <1 cm/s difference) and a maximum change of  
296 1.3 cm/s. A table of comparisons of these velocity estimations for each wave condition used  
297 in the flume is also included in Table S1 (line 35).

298 Based on the above relationship, we do not deem it necessary to re-run flume analyses  
299 using linear wave theory in place of the Soulsby Cosine Approximation.

300 P6, Line 19–20. The last statement on this page is very concerning: "Wave orbital velocities  
301 obtained in the flume were comparable to those measured in the field, hence scaling of the  
302 analyses was not required." As I explained above, the forces on the rubble are the relevant  
303 quantity that should be compared in the lab vs the field, and related to rubble motion. The  
304 velocities can be the same but if other important parameters are different (e.g., wave period)  
305 then direct comparisons of laboratory and field results will not be possible. Careful  
306 consideration of scaling is always required when relating lab flume experiments and the  
307 field situation.



308 Our response to the reviewer's general comment addresses this concern. As pointed out by  
309 the reviewer, total force depends on both the inertia force component and drag force  
310 component, and while the inertia component is dependent on velocity and wave period, the  
311 drag component is only dependant on the velocity (see equations outlined above). Thus,  
312 where conditions are determined to be drag dominated, rubble movement only depends on  
313 the velocity. As outlined in our response above, our investigation found minor issues with  
314 inertia becoming potentially significant at very low velocities in the flume, and some rubble  
315 pieces (18 cases) transporting in those conditions, but the contribution of inertia forces to  
316 total force in these cases was relatively small. Furthermore, the 50% threshold of  $\geq 0.3$  m/s  
317 represent wave conditions that are drag dominated as in the field. Thus, despite differences  
318 in the wave period between the field and flume, meaningful comparisons of these movement  
319 thresholds can be made. Since inertial forces are negligible at the 50% and 90% thresholds,  
320 the laboratory experiments do not have scale effects, since the coral rubble has the same  
321 scale in the laboratory and field and the velocity and Reynolds numbers therefore also have  
322 the same magnitudes.

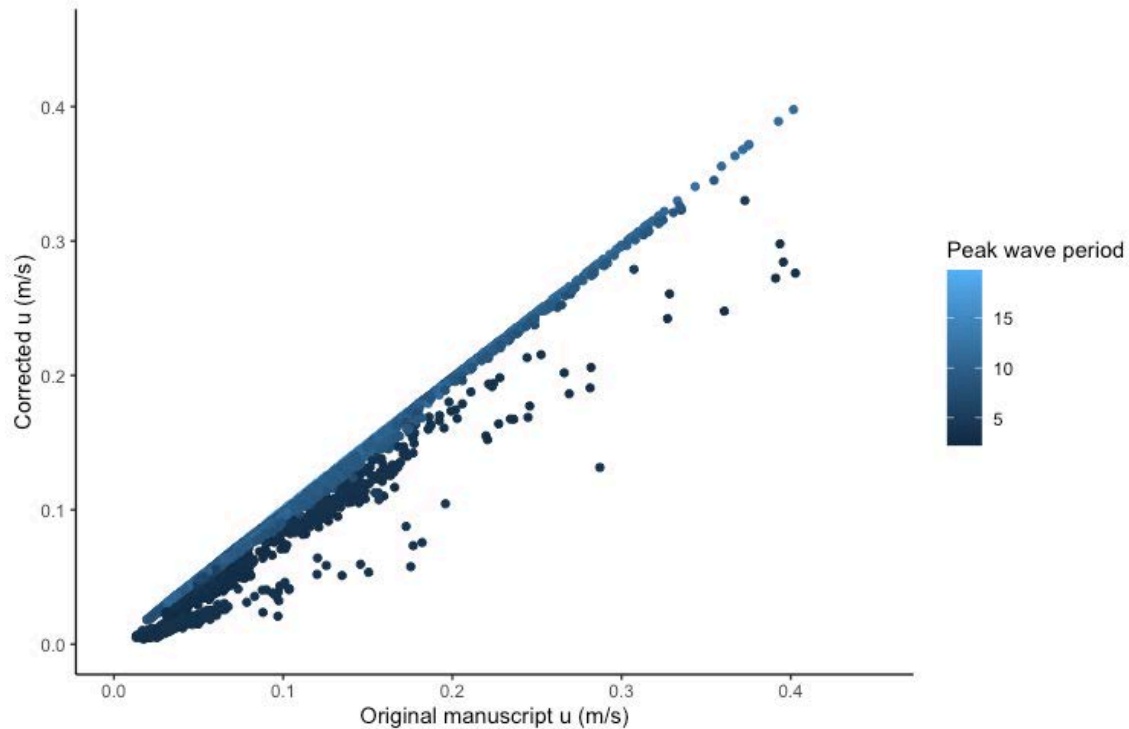
323 P8. Line 10. Unclear that the shallow water approximation is valid here for computing  
324 wavenumber  $k$ . There is readily available code available to calculate  $k$  from frequency and  
325 depth using the general/complete linear wave theory dispersion relation.

326 We thank the reviewer for this comment and agree that in some circumstances where the  
327 wave period is very short, the shallow water approximation should be avoided. We have now  
328 solved the dispersion relation to calculate the wave number ( $k$ ), and the near-bed orbital  
329 velocities in the field have been updated using the new  $k$  values. This is outlined in the  
330 manuscript as below:

331 "Pressure was converted to depth, and wave spectra for each 30-minute run were calculated between 0.0033-0.33  
332 Hz using the Welch method for computing power spectral densities from 3600 sample records, to obtain significant  
333 wave height ( $H_s$ ) and peak wave period ( $T_p$ ). The near-bed wave orbital velocity ( $U$ ) was then estimated for each  
334 30-minute run using linear wave theory using Eq. (3).

335 (3)  $U = \frac{H_s}{2 \sinh(kh)} \cdot \frac{2\pi}{T_p}$  where the wave number ( $k$ ) was determined by solving Eq. (4)  
336 (4)  $\omega^2 = gk \sinh(kh)$  where  $\omega$  is the wave radian frequency ( $2\pi/T_p$ ),  $h$  is water depth, and  $g$  the  
337 acceleration due to gravity."

338 A plot of the velocity as it appears in the original manuscript against the velocity using the  
339 wave number as calculated in the revised manuscript is shown below, showing that  
340 conditions where the shortest wave periods were observed (~4-5 s) result in the greatest  
341 change.



342

343 Results in Section 3.2, as well as figures 4, 5 and 6 of the revised manuscript have been  
 344 updated based on the updated analysis. The analysis of 50% threshold was found to have  
 345 changed slightly from 0.34 m/s to 0.3 m/s (making the updated 50% threshold in the field  
 346 more like that estimated for the flume), and the 90% threshold from 0.55 m/s to 0.75 m/s.  
 347 The following is included in the results section regarding the 90% threshold:

348 “We note however that the 90% threshold for transport is above the range of velocities measured in the field and  
 349 should thus be considered cautiously compared to the 50% threshold. We do not report the 50% or 90% thresholds  
 350 for flipping in the field for the same reason.”

351 P8. line 32. Unclear what is meant by peak wave orbital velocity here. Do you mean the  
 352 maximum 30-min significant wave height over the 3-day period? This is not truly the peak  
 353 wave orbital velocity, which would require going back to the original time series for each  
 354 burst.

355 The ‘peak’ wave orbital velocity in this manuscript is calculated based on the significant  
 356 wave height and the peak wave period from the wave spectrum, and we have selected the  
 357 fastest ‘peak’ wave orbital velocity per day for the regression with rubble movement. We  
 358 agree that the use of ‘peak’ in the referenced section of the manuscript may be confusing.

359 We have amended the text for clarity to now read:

360 “From the 30-minute runs across each 3-day period and site (144 each period and site), the fastest wave orbital  
 361 velocity (calculated from peak wave height and period) was selected for each day, to regress with observed rubble  
 362 movement on that day. A total of the 90 fastest wave orbital velocities were thus used in the analyses that included  
 363 all three days (1 velocity per day x 3 days x 15 sites x 2 seasons), and 30 were used in the analyses that included  
 364 the first day only (1 velocity for each ‘day 1’ x 15 sites x 2 seasons).”

365

366 P9. Results. Wave periods need to be reported and used appropriately in the analysis!

367 Tables of wave conditions in the flume and field, including average coral rubble diameter,  
368 wave height, period and water depth are now provided in the Supplementary Material as  
369 Tables S1 and S2. The additional text in the revised manuscript relating to this is pasted  
370 above from line 198. There is also a preamble to Table S1/S2 (line 34) explaining the  
371 equations used to calculate the inertia force component, as pasted below:

**Table S1/S2 pre-amble:** Assuming the drag and inertia coefficients have the same magnitude, the ratio of the maximum inertia force to the maximum drag force is given by Dean and Dalrymple (1991) as:

$$(1) \frac{F_I}{F_D} = \frac{\pi^2}{KC} = \alpha \quad \text{where } KC = \frac{uT}{\varnothing}; \text{ KC = Keulegan-Carpenter number, } u = \text{maximum orbital wave velocity, } T = \text{wave period } \varnothing = \text{rubble diameter}$$

Hence  $F_I = \alpha F_D$

The maximum total force is again given by Dean and Dalrymple (1991), noting that the drag and inertia forces are out of phase,

$$(2) F_T = F_D + \frac{F_I^2}{4.F_D} \quad \text{FT = maximum total force, FD = drag force, FI =inertia force}$$

which can be written as  $F_T = F_D + \frac{\alpha^2}{4} F_D$  or  $F_T = F_D + \frac{24}{KC^2} F_D$

The last term ( $\frac{24}{KC^2}$ ) gives the contribution of the inertia force to the total maximum force as a proportion of the drag force. We consider the inertia component to be potentially significant when it contributes more than 25% of the drag force to the total force. For example, when FI=FD, the contribution to the maximum total force from the inertia force is 0.25FD. It should be noted that this relationship is only valid for  $\frac{F_I}{F_D} < 2$ , and when  $\frac{F_I}{F_D} > 2$ , the maximum force is pure inertia (Dean and Dalrymple, 1991).

372

373 Fig 4. Bottom orbital excursion and accelerations should be shown also, for the reasons  
374 outlined in my General Comments

375 We have included a table of wave conditions used in the flume (Table S1 - line 35) and the  
376 field (Table S2 - line 42) in the Supplementary Material of the revised manuscript. These  
377 show the average coral rubble diameter, wave height, period, water depth, and  
378 corresponding velocities, inertial force component and bottom orbital excursions for all  
379 wave conditions used in determining the relationship between velocity and movement. As  
380 one of the key goals of this work is to inform management around reef restoration, we feel  
381 that the presentation of the results (figures) as a function of velocity is more broadly  
382 comprehensible to managers than are forces.